

Hybrid Inorganic–Organic Poly(carborane-siloxane-arylacetylene) Structural Isomers with In-Chain Aromatics: Synthesis and Properties

Manoj K. Kolel-Veetil,¹ Dawn D. Dominguez,¹ Christopher A. Klug,¹ Kenan P. Fears,¹ Syed B. Qadri,² Daniel Fragiadakis,¹ Teddy M. Keller¹

¹Chemistry Division, Naval Research Laboratory, Washington DC 20375

²Material Science & Technology Division, Naval Research Laboratory, Washington DC 20375

Correspondence to: M. K. Kolel-Veetil (E-mail: Manoj.kolel-veetil@nrl.navy.mil)

Received 21 November 2012; accepted 18 February 2013; published online 26 March 2013

DOI: 10.1002/pola.26653

ABSTRACT: Structural isomers of thermo-oxidatively stable poly(carborane-siloxane-arylacetylene) (PCSAA), namely, *m*-PCSAA and *p*-PCSAA, were synthesized by the reaction of the dimagnesium salts of *m*-diethynylbenzene or *p*-diethynylbenzene with 1,7-bis(chlorotetramethyldisiloxy)-*m*-carborane. The developed polymers have exceptional thermo-oxidative properties similar to their diacetylene counterpart poly(carborane-siloxane-acetylene), PCSA. Thermal treatment of either of the PCSAAs results in a fully crosslinked thermoset by 500 °C resulting from the cycloaddition reactions involving the acetylene and aryl functionalities and subsequent formation of bridging disilylmethylene entities as discerned from Fourier transform infrared, ¹³C and ²⁹Si solid-state NMR, and XPS studies. X-ray diffraction analysis revealed that the thermosets obtained from *p*-PCSAA possess enhanced crystallinity when compared to that obtained from *m*-PCSAA possibly due to more efficient packing

interactions of the *p*-diethynylbenzene groups during thermoset formation. The presence of the aryl groups in the backbone of the PCSAAs' chains appeared to have enhanced the storage and bulk moduli of their thermosets when compared to the thermoset of PCSA. Dielectric studies of *m*-PCSAA and *p*-PCSAA revealed segmental relaxation peaks, α , above their glass transition temperatures with *p*-PCSAA exhibiting a broader peak with a slower relaxation rate than *m*-PCSAA. © 2013 Wiley Periodicals, Inc. *J. Polym. Sci., Part A: Polym. Chem.* **2013**, *51*, 2638–2650

KEYWORDS: acetylene; addition polymerization; arylacetylene; carboranylenesiloxane; carborane; cycloaddition; crosslinking; dielectric properties; disilylmethylene; glass transition; high temperature materials; infrared spectroscopy; inorganicorganic; network; mechanical properties; NMR; PCSA; PCSAA; siloxane; thermal properties; X-ray

INTRODUCTION Although many examples of carboranylenesiloxane polymers with aromatic pendant groups have been reported¹ since the discovery of carboranylenesiloxane polymers in the late 1970s,² there are only a few reports of carboranylenesiloxane polymers that contain aromatic groups in the polymer backbone. Of the five examples that are available, three are network polymers,³ and in the remaining two linear polymers, the aromatic group exists in a copolymer unit with either a sulfone group⁴ or a silane group.⁵ The interest in *in-chain* incorporation of aromatic groups in a polymer stems from the fact that it increases the melting temperature and/or glass transition temperature of the resulting polymer due to chain stiffening and alterations in the conformation of the polymer chains.⁶ The insertion of an aryl group in a known carboranylenesiloxane polymer, therefore, can be expected to alter its material characteristics especially with regard to its mechanical properties. Additionally, if groups such as alkynes are connected immediately to the incorporated aryl group,

they can facilitate new crosslinking pathways such as cycloaddition reactions that involve both groups.⁷ In this regard, a group of carboranylenesiloxane polymers, namely, poly(carborane-siloxane-acetylene), PCSA (Fig. 1), developed at the Naval Research Laboratory that contain diacetylenes as crosslinking entities is of interest.⁸ When PCSA is thermally cured, the diacetylene groups in the polymer backbone function as sites of crosslinking via topochemical 1,4-polymerization.⁹ Upon formation of crosslinked domains, the resulting thermoset material is tough and somewhat brittle. The insertion of aryl group in between the two acetylene units of the diacetylene group in PCSA should expectedly facilitate the alluded cycloaddition reaction rather than only the 1,4-polymerization or other crosslinking reaction chemistry¹⁰ that involves only the acetylenes during thermoset formation. The inclusion of the aryl rings in the backbone of the PCSA polymer should also stiffen the resulting polymer thereby yielding tougher thermoset networks. To this end, two aromatic group-

Additional Supporting Information may be found in the online version of this article.

© 2013 Wiley Periodicals, Inc. [†]This article is a U.S. Government work, and as such, is in the public domain in the United States of America.

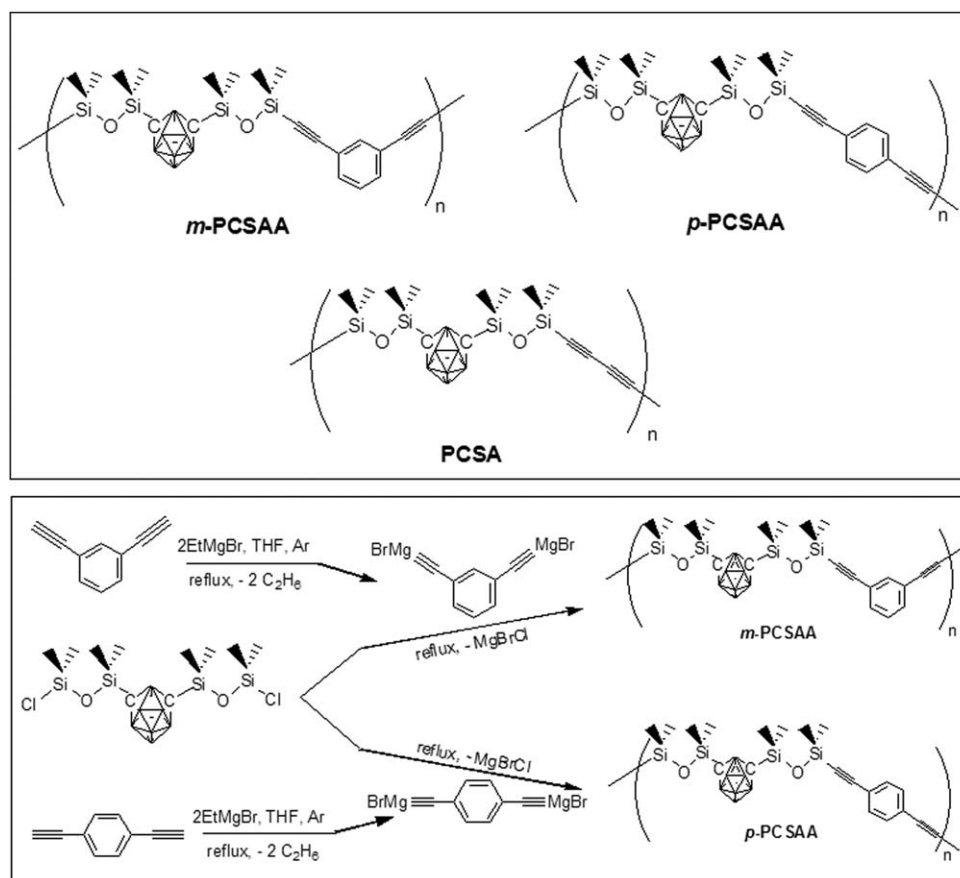


FIGURE 1 Top box: The in-backbone aromatic group-containing carboranylenesiloxanes *m*-PCSAA and *p*-PCSAA of this study and their diacetylene counterpart, PCSA. Bottom box: Synthetic schemes for *m*-PCSAA and *p*-PCSAA.

containing structural isomers, namely, *m*-PCSAA (poly (carborane-siloxane-arylacetylene)) and *p*-PCSAA (Fig. 1), were developed by the respective reaction of the dimagnesium salts of 1,3-diethynylbenzene (*m*-DEB) and 1,4-diethynylbenzene (*p*-DEB), with the difunctional carboranylenesiloxane monomer, 1,7-bis(chlorotetramethyldisiloxy)-*m*-carborane (BCTMDS-*m*-C). The synthesis, crosslinking chemistry and other material properties of the two polymers are described below.

RESULTS AND DISCUSSION

Characterization of the PCSAAs

m-PCSAA and *p*-PCSAA were synthesized by the reaction between the Grignard derivative of the respective DEB, with two terminal Grignard functionalities, and the bifunctional carboranylenesiloxane BCTMDS-*m*-C (Fig. 1). Both Grignard reactions proceeded efficiently and produced the products in high yields (>98%). In reactions with BCTMDS-*m*-C, while *m*-DEB's Grignard reagent produced a viscous pale brownish red product, *p*-DEB's Grignard reagent produced a pale brown product that was even more viscous and sticky than the former. The molecular weights of the two polymers were compared with that of the PCSA polymer using gel permeation chromatography (GPC) (Table 1 and Supporting Information Fig. S1). The molecular weights of the three

polymers were found to be reasonably similar. The higher M_n and M_w of *p*-PCSAA when compared to that of *m*-PCSAA suggested some differences in the degrees of reaction and the associated chain growths leading to the two polymers. In contrast, M_n of *m*-PCSAA and PCSA were found to be quite similar. The mechanical properties of these two polymers were analyzed by dynamic mechanical analysis (DMA) (*vide infra*). Furthermore, the thermal stabilities of the two PCSAAs were similar and were nearly identical to that of PCSA.⁸ The thermogravimetric analysis (TGA) thermograms in argon of the two polymers almost follow the same trace to 1200 °C except in the range 200–500 °C where there is an inversion in the traces, the origin of which is not clear (Fig. 2). This causes *p*-PCSAA to have a higher temperature at 5% weight loss than *m*-PCSAA (400 vs. 349 °C). The weight loss can be attributed to the loss of some unreacted

TABLE 1 GPC Molecular Weight Data for *m*-PCSAA, *p*-PCSAA, and PCSA

Polymer	M_n (g/mol)	M_w (g/mol)
<i>m</i> -PCSAA	5,792	7,862
<i>p</i> -PCSAA	7,584	10,944
PCSA	5,484	8,915

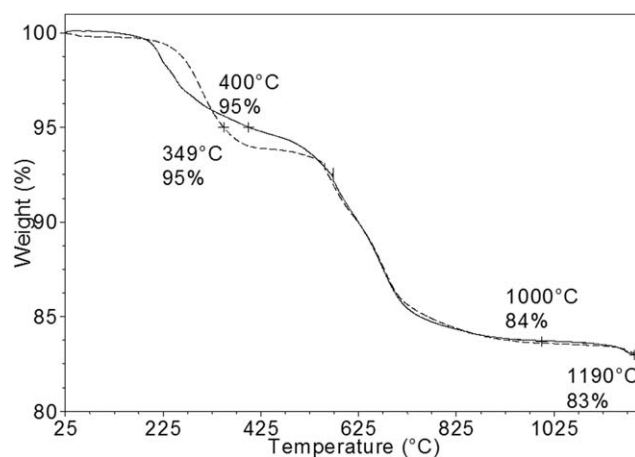


FIGURE 2 TGA thermograms in argon of *m*-PCSAA (dashed) and *p*-PCSAA (solid).

DEB and/or low molecular weight cyclic oligomers that might have formed especially during the synthesis of *m*-PCSAA. Both *m*-PCSAA and *p*-PCSAA produce ceramics with a char yield of 84% at 1000 °C which is nearly the same (i.e., a ceramic yield of 85%) as that observed with PCSA under similar conditions.⁸ The two ceramics further lose only another percent of their weight up to 1200 °C. Thus, the insertion of the isomeric aryl ring in the diacetylene unit does not seem to have detrimentally impacted the thermal stability of the resulting polymers. Coincidentally, the char yield in air at 1000 °C of both *m*-PCSAA and *p*-PCSAA was 93% and was similar to that of PCSA. In the DSC thermograms of *m*-PCSAA and *p*-PCSAA, two exotherms were observed; a moderate one peaking around 290 °C and a strong one peaking around 395 °C (Fig. 3). Based on ¹³C and ²⁹Si solid-state NMR and Fourier transform infrared (FT-IR) studies of similarly obtained, thermally treated samples of the two polymers (*vide infra*), it appears that the first moderate exotherm originates from the consumption of the acetylene units of the DEB entities and the second strong exotherm arises from methylene bridge formation from adjacent Si-CH₃ entities that are brought closer in proximity upon the cycloaddition reaction, both of which will be

discussed below. Two endothermic peaks, at 121 and 150 °C, were also observed in the DSC thermogram of *p*-PCSAA and are believed to be due to the melting transition of some localized crystalline environments in *p*-PCSAA due to a propensity for crystallization in this system when compared to *m*-PCSAA, which was also corroborated by the X-ray diffraction (XRD) data (*vide infra*).

Characterization of *p*-PCSAA and *m*-PCSAA polymers by NMR spectroscopy revealed that they possess nearly identical resonances in their ²⁹Si NMR spectra at around 1.6 and -16.8 ppm suggesting the presence of only two types of Si atoms (Fig. 4). This is in agreement with their structures that are expected to contain only two sets of Si atoms. Each of these Si atom types possesses two methyl groups, that is, as a =Si-(CH₃)₂ entity; however, each one is connected to different atoms/groups at its third and fourth valencies. In the first type, the third and the fourth valencies are occupied by an acetylene carbon of the DEB group and an oxygen atom of the siloxyl group, respectively. The corresponding connectivities in the second type are to a carbon atom of the carborane cluster and an oxygen atom of the siloxyl group, respectively. Because of the enhanced electronegative character of the *sp*-hybridized carbon of the DEB's acetylene group, the resonance at -16.8 ppm should belong to the first type of Si atoms (note: minor resonances present at 0.7 and -16.4 ppm in the ²⁹Si NMR of *m*-PCSAA are presumed to be derived from a minor fraction of cyclic oligomers formed during its synthesis). Similarly, *m*-PCSAA and *p*-PCSAA exhibited comparable multiplets between -3 and -15 ppm in their ¹¹B NMR spectra. Even though similar resonances were observed for the carbon atoms in the methyl, *m*-carborane and alkyne groups in the ¹³C NMR spectra of *m*-PCSAA and *p*-PCSAA, distinct resonances were present for the aromatic carbons of the respective DEB entity (Fig. 5). Although resonances for the aromatic carbons were observed at 135.25, 132.21, 128.41, and 122.95 ppm for *m*-PCSAA suggesting the presence of four distinct ring carbons, only two resonances at 132.01 and 123.21 ppm were present for *p*-PCSAA indicating two types of aromatic carbons; all of which are consistent with their structures. As expected, in *p*-PCSAA's case, the resonance for the substituted ring carbons (two in total) at 123.21 ppm was of reduced intensity

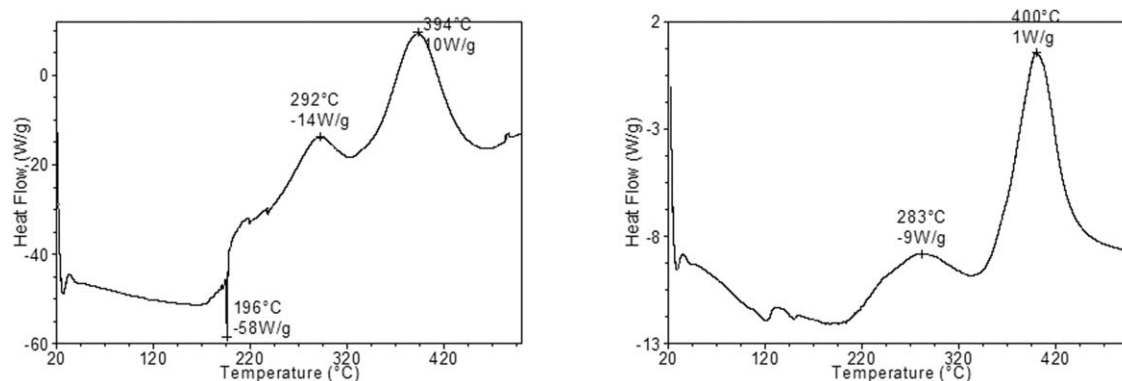


FIGURE 3 DSC thermograms in argon of *m*-PCSAA (left) and *p*-PCSAA (right).

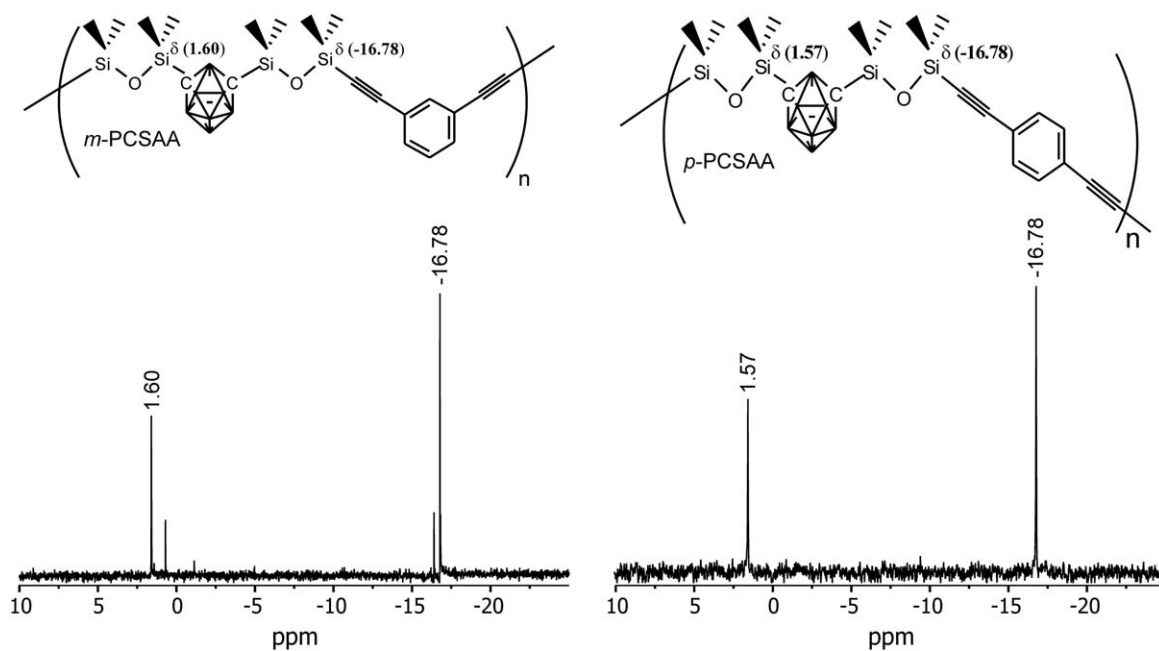


FIGURE 4 ^{29}Si NMR of *m*-PCSAA (left) and *p*-PCSAA (right).

compared to that of the resonance for the unsubstituted ring carbons (four in total) at 132.01 ppm. The observed distinction with regard to the number and intensity of resonances of the aromatic carbons, and the presence of similar ^{29}Si chemical shifts were used as “spectroscopic markers” in deciphering the prevailing crosslinking mechanism/s in the two polymers (*vide infra*). Similar differences were also observed for the aromatic groups in the ^1H NMR spectra of *m*-PCSAA and *p*-PCSAA.

The FT-IR spectra of *p*-PCSAA and *m*-PCSAA are quite similar, especially, in the higher wavenumber region (4000–1500 cm^{-1}). However, remarkable differences are evident in the fingerprint region (1600–500 cm^{-1}) (Fig. 6). The differences arise from the distinct in-plane stretching modes, that is, $\nu(\text{C}-\text{C})$, of *m*-DEB and *p*-DEB.¹¹ Thus, the $\nu(\text{C}-\text{C})$ modes appear at 1509, 1498, and 1411 cm^{-1} in the spectrum of *p*-PCSAA whereas they appear at 1596, 1570, 1477, and 1411 cm^{-1} for *m*-PCSAA. It was also apparent from the FT-IR

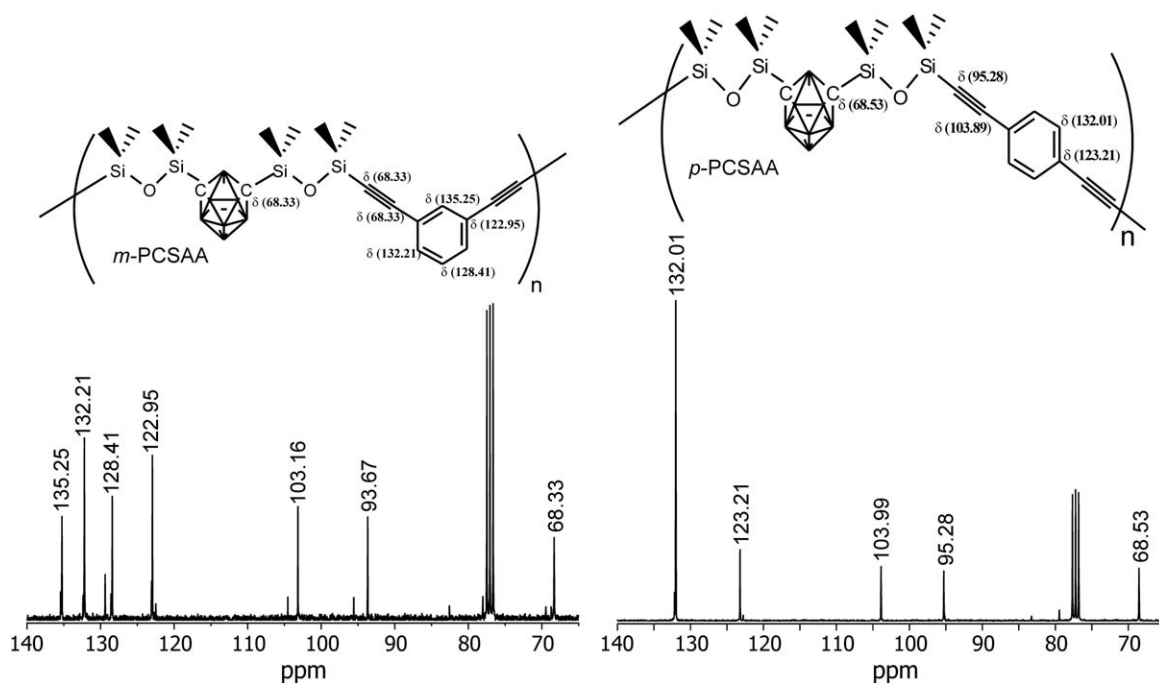


FIGURE 5 ^{13}C NMR of *m*-PCSAA (left) and *p*-PCSAA (right).

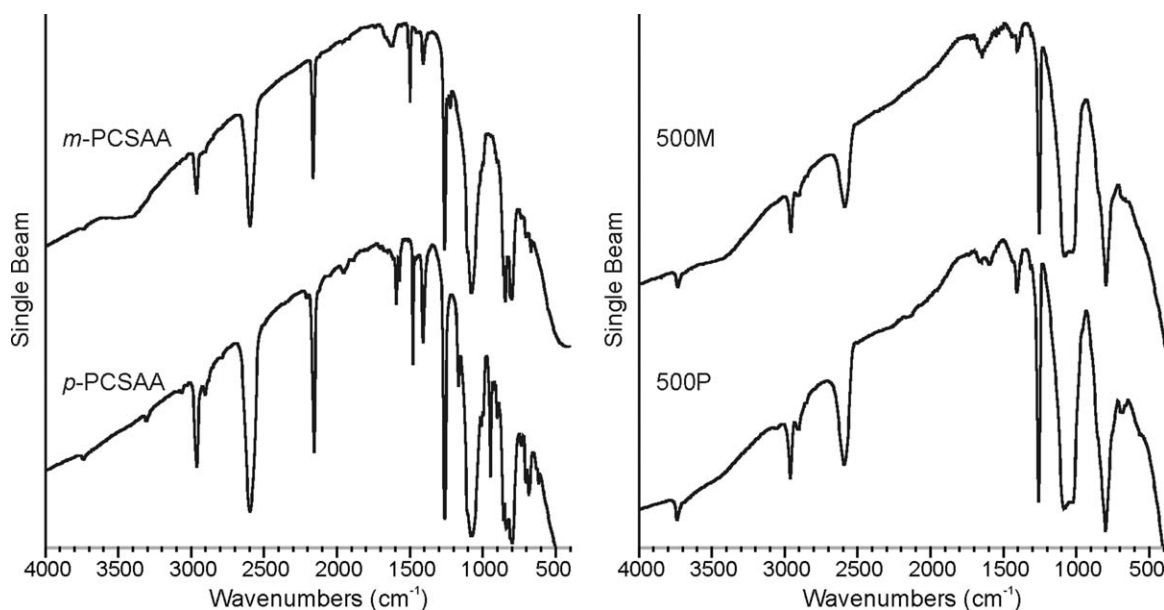


FIGURE 6 FT-IR spectra of (left) *m*-PCSAA (top) and *p*-PCSAA (bottom); and (right) of the thermosets formed at 500 °C of *m*-PCSAA (top) and *p*-PCSAA (bottom).

spectrum of *m*-PCSAA that some of its chains had $\equiv\text{C}-\text{H}$ chain terminations associated with the DEB groups as inferred from the $\nu(\equiv\text{C}-\text{H})$, $\beta(\text{C}-\text{H})$, and $\gamma(\text{C}-\text{H})$ stretching modes at 3303, 1167, and 947 cm^{-1} , respectively.¹² The absence of corresponding modes in the spectrum of *p*-PCSAA suggested that its chain terminations were mainly of the Si-OH type. The difference in the chain terminations in the two polymers is likely due to the difference in the degree of reactivity during the synthesis of the two polymers, as evident from their molecular weights, with possibly different chain growth scenarios. Furthermore, the presence of an absorbance at 3738 cm^{-1} in both resins implied that there were isolated Si-OH entities in the resins.¹³

Studies of the Curing Pathways in the PCSAAs: Is it by 1,4-Polymerization of the Acetylenes and/or by the Cycloaddition Reaction of the DEB Groups?

It was of interest to determine the nature of the crosslinking mechanism/s in the two PCSAAs due to the presence of the isomeric DEB groups. As alluded, in PCSA the diacetylene groups crosslink by the topochemical 1,4-addition reaction of such groups. Similarly, crystals of *p*-DEB are known to undergo UV or γ -radiation-induced low-temperature solid-state polymerization through their acetylene groups (Scheme 1) via a radical mechanism to yield stereo-regular polymers.¹⁴ As thermosets formed from *p*-PCSAA exhibited signs of crystallinity in their XRD spectra in contrast to the ones formed from *m*-PCSAA (*vide infra*), it was interesting to determine whether the crosslinking in only *p*-PCSAA occurred via its acetylene groups as in the UV or γ -radiation-induced low-temperature solid-state polymerization or whether the crosslinking in both *p*-PCSAA and *m*-PCSAA occurred by a cycloaddition mechanism as illustrated in Scheme 1. This should also answer whether the greater

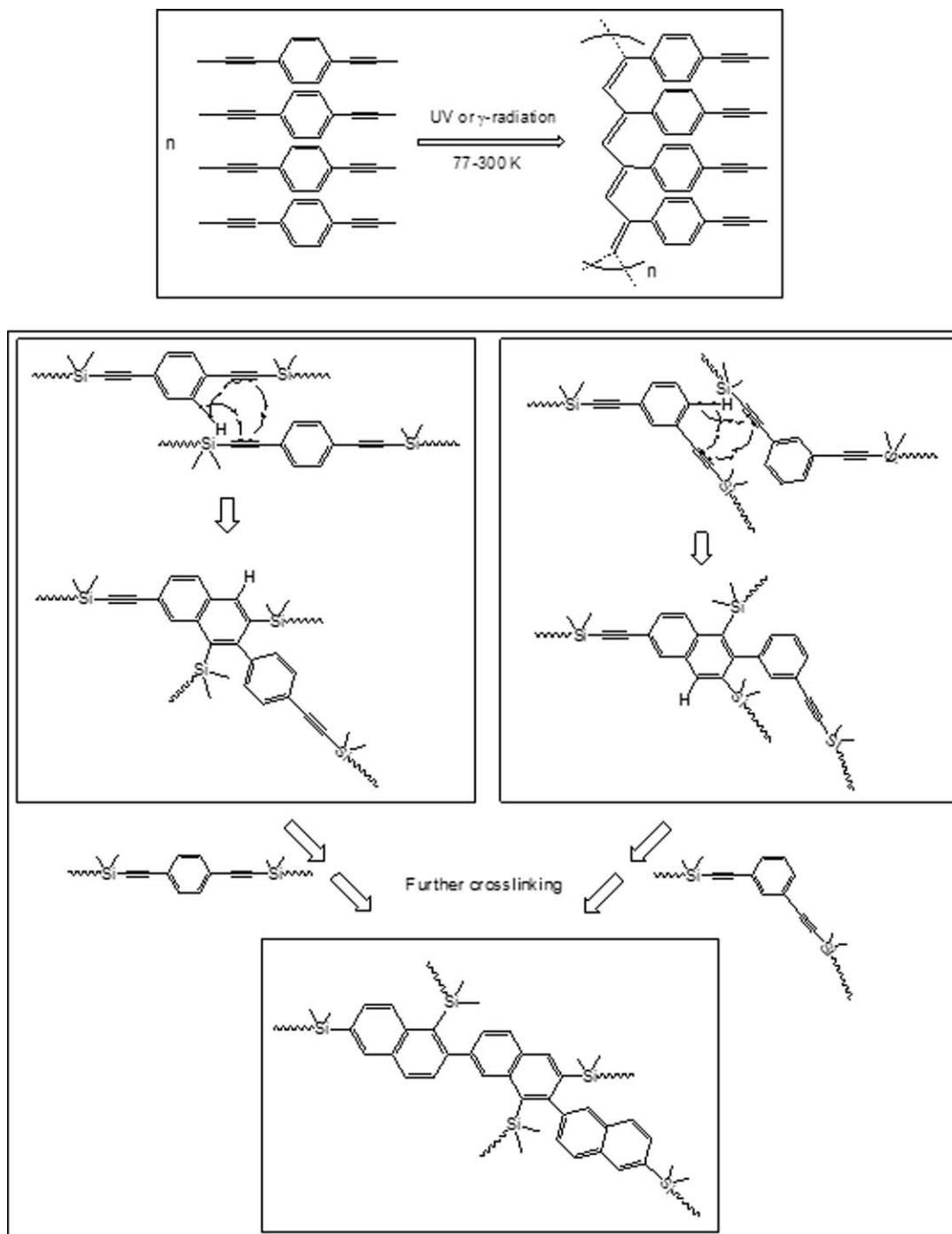
propensity for stacking of the *p*-DEB groups had any impact on the nature of the crosslinking in *p*-PCSAA when compared to *m*-PCSAA, as discussed below.

XRD Studies

For performing XRD evaluations, identical samples of *m*-PCSAA and *p*-PCSAA were thermally treated to 350, 400, 450, and 500 °C under argon in aluminum planchets under similar conditions (note: the respective samples are denoted as 300M, 400M, 450M, or 500M for *m*-PCSAA or as 300P, 400P, 450P, or 500P for *p*-PCSAA wherein the number denotes the temperature of thermal treatment and the suffix M or P denotes the nature of the DEB). 2θ measurements were performed in the range 20–80° to determine the extent of crystallinity in the two sets of samples (Fig. 7). The analysis revealed an absence of crystallinity in any of the *m*-PCSAA samples suggesting that even after thermoset formation the crosslinked domains only had amorphous characteristics. In contrast, for 350P, 400P, and 450P, relatively broad peaks were observed at 2θ values of 34, 42, and 31°, respectively, with *d*-spacing values of 2.643, 2.110, and 2.643, suggesting the formation of small crystalline domains in the thermosets. In comparison, 500P exhibited a sharp peak at 31.5° with a *d*-spacing of 2.838 hinting that the crystalline entities in this sample were comparatively larger in size than the ones in the thermosets obtained at lower temperatures. This implied that at higher temperatures the completion of the crosslinking occurred with the production of crystalline domains with a longer range order.

¹³C and ²⁹Si NMR Solid-State NMR Studies

The fates of the alluded “spectroscopic markers,” in the respective ¹³C and ²⁹Si NMR spectra of the thermally treated samples of *m*-PCSAA and *p*-PCSAA resins, were followed to determine the nature of the crosslinking pathways in



SCHEME 1 (Top box) Low-T, UV or γ -radiation initiated polymerization of *p*-DEB; Cycloaddition reactions of *p*-DEB (Middle, left box) and of *m*-DEB (Middle, right box), showing one possible mode of approach of the polymer chains, leading to the same cross-linked, cycloaddition product (Bottom box).

operation in these systems. The multiplicity in the aromatic resonances of *m*-PCSAA was persistent in the ^{13}C NMR solid-state spectrum of the 300M sample as obvious from the broader peak for such resonances. In contrast, for the 300P sample, the sharper signal at 132 ppm of the unsubstituted ring carbons was still apparent in its ^{13}C NMR solid-state spectrum (Fig. 8). The acetylene resonances were also still

observable for both 300M and 300P. However, by 350 °C, in both 350M and 350P, the resonances of the acetylene entities had disappeared and the distinguishable aromatic resonances of both polymers appeared to be converging to a similar shape. This suggested that as the acetylenes got consumed during the thermal crosslinking process, their reactions produced crosslinked structures with similar aromatic

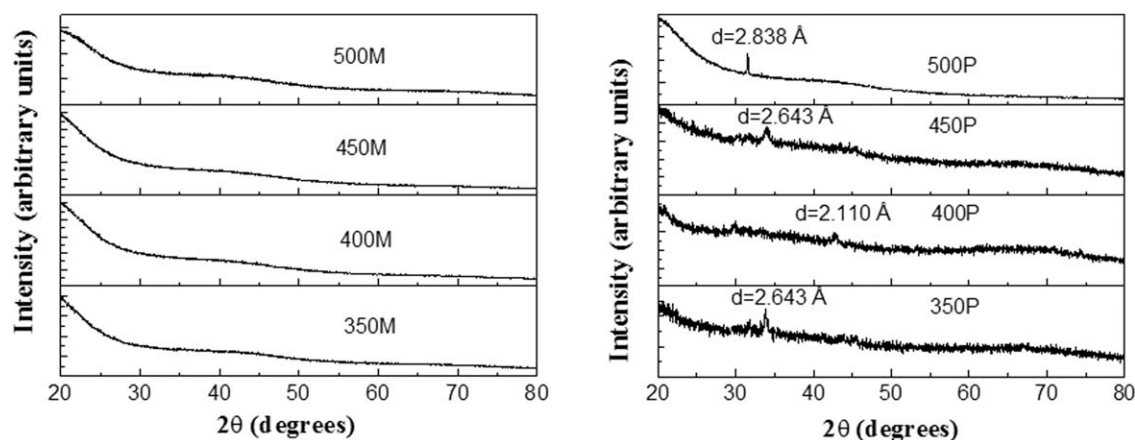


FIGURE 7 XRD spectra of the thermally treated samples of *m*-PCSAA (left) and *p*-PCSAA (right).

architectures. This can only be possible if a pathway such as a cycloaddition reaction (Scheme 1) is in operation as it would produce similar naphthyl-type crosslinked entities in both *p*-PCSAA and *m*-PCSAA that would be indistinguishable in their solid-state NMR spectra. If a reaction mechanism such as the acetylene polymerization (Scheme 1) as observed with the crystals of *p*-DEB were to be occurring in *p*-PCSAA, the characteristic aromatic feature such as the sharper resonance around 132 ppm should have persisted in its thermally crosslinked samples. By 500 °C, the ^{13}C NMR spectra of the thermosets of both polymers were found to be nearly

identical confirming the occurrence of the cycloaddition mechanism during crosslinking of the two resins.

The consumption of the acetylene groups during the cycloaddition reaction when both *p*-PCSAA and *m*-PCSAA are thermally crosslinked can also be deduced from the ^{29}Si NMR spectra of the samples. The complete disappearance of the Si resonance at -16.8 ppm belonging to Si atoms attached to an acetylene group (Fig. 8) supports this. As the acetylenes become consumed by 350 °C and the resonance of the Si atoms at -16.8 ppm attached to the acetylenes progressively

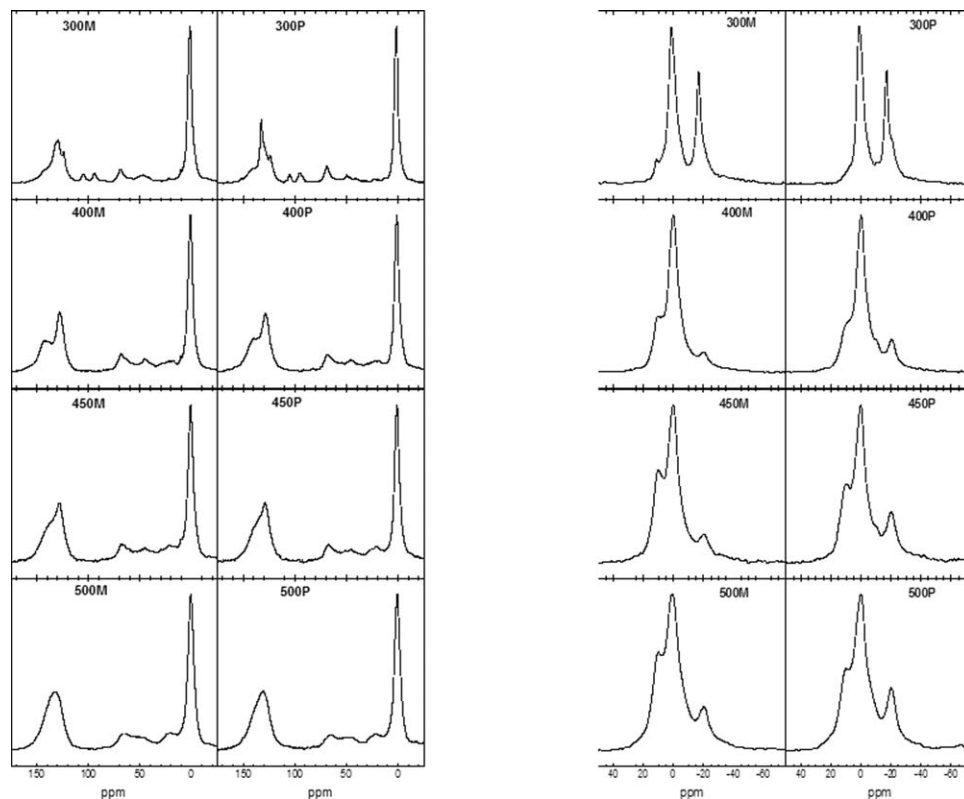
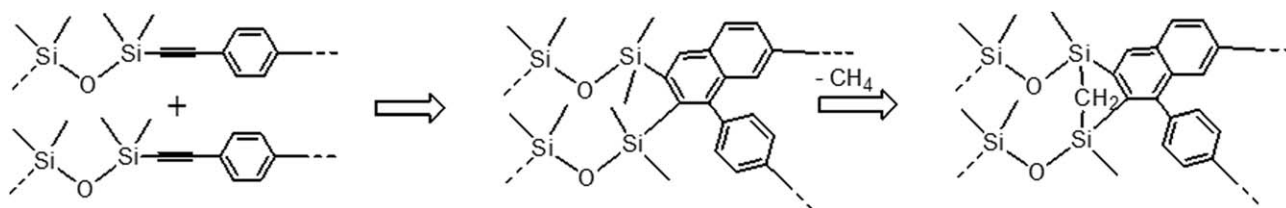


FIGURE 8 ^{13}C (left) and ^{29}Si (right) solid-state NMR spectra of various thermally treated samples of *m*-PCSAA and *p*-PCSAA.



SCHEME 2 Mechanism of disilylmethylene bridge formation.

disappears, there is a concomitant growth of a resonance around 10 ppm belonging to a new set of Si atoms that is produced from the acetylene-attached Si atoms that underwent the transformation. This new group of $(\text{CH}_3)_2\text{Si}=\text{C}$ entities is still connected by an oxygen atom of the siloxane unit at its third valency; however, this new group is now connected to a ring carbon of the newly formed naphthyl-like group at its fourth valency instead of the original acetylene carbon. It is reasonable that the lesser electronegative nature of the naphthyl group shifts the resonance of this new group of silicon atoms upfield by ~ 15 ppm. Furthermore, a fortuitous reemergence of a Si resonance at around -16.8 ppm, that is, at the same resonance as the consumed Si atoms, should be attributed to another new type of Si species based on NMR analysis, and corroborating FT-IR analysis discussed in the following section. As both FT-IR and ^{13}C solid-state NMR analyses suggest the complete disappearance of the acetylene groups by 400°C , this new resonance is believed to be that of Si atoms that are bridged by methylene groups. Such methylene groups can be derived from the reactions of adjacent Si-bound methyl groups resulting in the expulsion of CH_4 leading to such bridging coordination between two adjacent silicon atoms (Scheme 2). It has been reported that such reactions can occur, at even lower temperatures than the ones used here, in thermosets with a high degree of crystallinity as the $=\text{Si}-(\text{CH}_3)_2$ groups are rendered close in proximity, such as in the system $-\text{[Si}(\text{CH}_3)_2-\text{C}\equiv\text{C}-\text{C}\equiv\text{C}]_n-$.¹⁵ In *m*-PCSAA and *p*-PCSAA when the cycloaddition reaction proceeds, it results in two methyl groups on nearby Si atoms being brought closer, as depicted in Scheme 2, resulting in the formation of methylene bridges subsequent to the expulsion of methane. Fortuitously, the combined electronegativities of the bridging methylene group and the naphthyl-type carbon atom seem to be of an equal value as that of the combined electronegativities of an sp carbon of the acetylene group and the transforming Si-bound methyl group which are consumed, thus placing the resonance of this new set of Si atoms near the original resonance of the initial Si atoms that underwent the transformation. As the crystalline order is greater in 400P, 450P, and 500P than in 400M, 450M, and 500M, it is possible that the disilylmethylene formation becomes more favored in the former samples, thus explaining the higher signal intensity for such Si atoms in those samples. However, it could also be that the spin-lattice relaxation time (T_1) of this new group of Si atoms is greater in the *m*-PCSAA samples than in the *p*-PCSAA samples resulting in the differences in the intensity of the resonances.

FT-IR Studies

As the PCSAA resins have distinct peaks in the fingerprint region, the hallmark in-plane vibrations of the *meta* or *para* substituted aryl rings should have persisted in the FT-IR spectra of the thermosets if a mechanism involving only acetylene units were in operation during crosslinking. The analysis of the FT-IR spectra of the various thermosets (Supporting Information Fig. S2) revealed that the acetylenes are completely consumed by 400°C in agreement with the ^{13}C solid-state NMR data. The distinct in-plane stretching modes ($\nu(\text{C}-\text{C})$) of *m*-DEB and *p*-DEB observed in the parent resins were found to be absent in the thermoset samples. The remarkable similarity in the two spectra suggested that the curing process in operation produced very similar networks from both *p*-PCSAA and *m*-PCSAA, such as from a cycloaddition reaction (Scheme 1). In fact, the observed vibrations at 1653 , 1604 , 1446 , and 1412 cm^{-1} for 500M and at 1653 , 1446 , and 1414 cm^{-1} for 500P (Fig. 6) suggested that naphthalene-like structures as shown in Scheme 1 were produced by cycloaddition reactions in the two resins.¹⁶ The difference/s in the peaks between 1660 and 1600 cm^{-1} in the two thermoset samples point to differences in the disposition of the groups connected to the naphthalene-like structures arising from the cycloaddition reactions. The growth of a sharper peak around 1040 cm^{-1} in both sets produced above 350°C suggested that once the cycloaddition reaction occurred, the $=\text{Si}(\text{CH}_3)_2$ groups of neighboring polymer chains are brought sufficiently close together from which the proposed disilylmethylene species formation occurs (Scheme 2). Bridging disilylmethylene groups are known to produce strong bands that are sharper in contrast to $-\text{Si}-\text{O}-\text{Si}-$ bands in the range 1080 – 1040 cm^{-1} .¹² Hence, the retention of the Si-O-Si band around 1080 cm^{-1} and the growth of the 1040 cm^{-1} band in the samples treated above 350°C that underwent the cycloaddition reaction suggest that both $-\text{Si}-\text{O}-\text{Si}-$ and disilylmethylene species are present in these thermosets. The growth of the absorbance at 3738 cm^{-1} in the thermally treated samples also implied that additional isolated Si-OH groups were produced during the crosslinking process the cause of which is yet to be determined.¹³

XPS Studies

XPS analysis provides information on the binding energies of various atomic orbitals from which the progression of chemical transformations in material systems can be obtained. In the Si 2p region of the XPS spectra for both *p*-PCSAA and *m*-PCSAA, there was a single, narrow peak

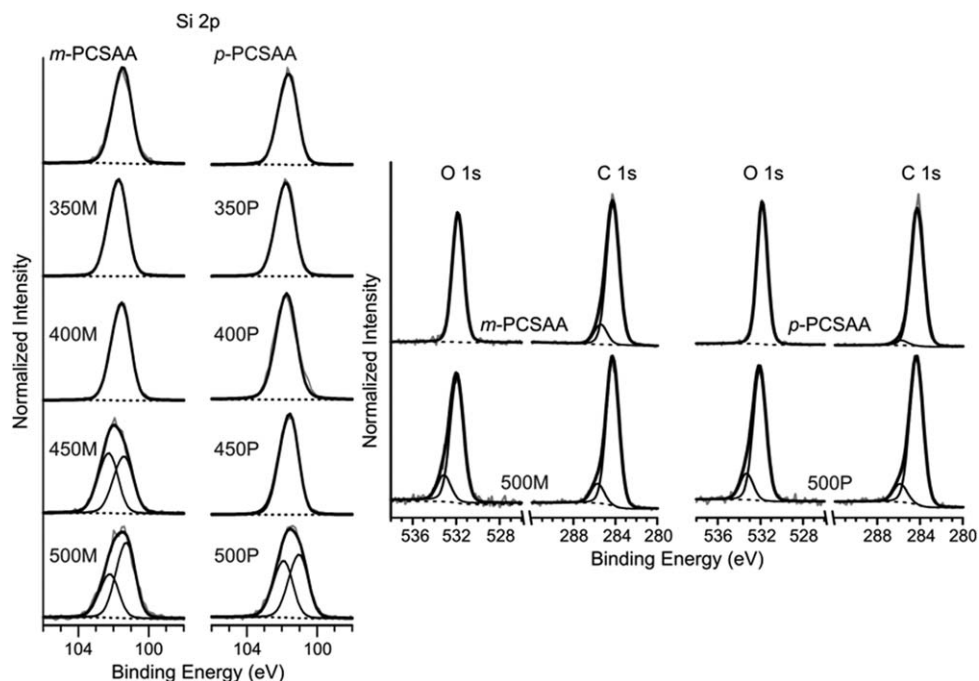


FIGURE 9 High-resolution XPS spectra of the Si 2p, C 1s, and O 1s regions of *m*-PCSAA and *p*-PCSAA before and after heat treatment. The spectra were normalized by the maximum peak intensity of each spectrum for ease of comparison.

(FWHM = 1.1–1.2 eV) (Fig. 9) centered near BE = 101.5 eV that corresponds with SiOC_3 , that is, a silicon that is bonded to one oxygen and three carbons.^{17,18} Since both sets of Si atoms, as discussed, have connectivities to three carbon atoms and an oxygen atom, it appears that a distinction in their binding energy is not apparent in the XPS spectra, even though their ^{29}Si solid-state NMR spectra exhibited distinct resonances. The Si 2p peak of each resin broadened with increasing temperature of heat treatment indicating that the nature of the chemical states of Si atoms in the thermosets was changing on progression of crosslinking. The chemical states of oxygen in the two resins, and in 500M and 500P appeared similar. Although differences were observed in the C 1s region of the *p*-PCSAA and *m*-PCSAA, there is little difference in the C 1s region between 500M and 500P, which is consistent with the results from FT-IR and NMR spectroscopic data.

The valence band XPS spectra of the polymer resins before and after the various heat treatments are shown in Figure 10. All of the thermoset samples exhibit strong bands in the C 2s and C 2p regions that correspond to the molecular orbitals associated with C–C bonds and $p\pi$ molecular orbitals,^{19–21} respectively, as well as a band in the O 2s region. The binding energies of the bands in the O and C 2s regions are fairly consistent across all of the samples which indicate that no new C–O species are formed during heat treatment of the resins. Although the changes in the O 2s and C 2s regions are minimal, the profile of the bands in the C 2p region shifts as the resins are thermally crosslinked, which happens as a result of the rearrangement of π bonds during intermolecular cycloaddition reactions.

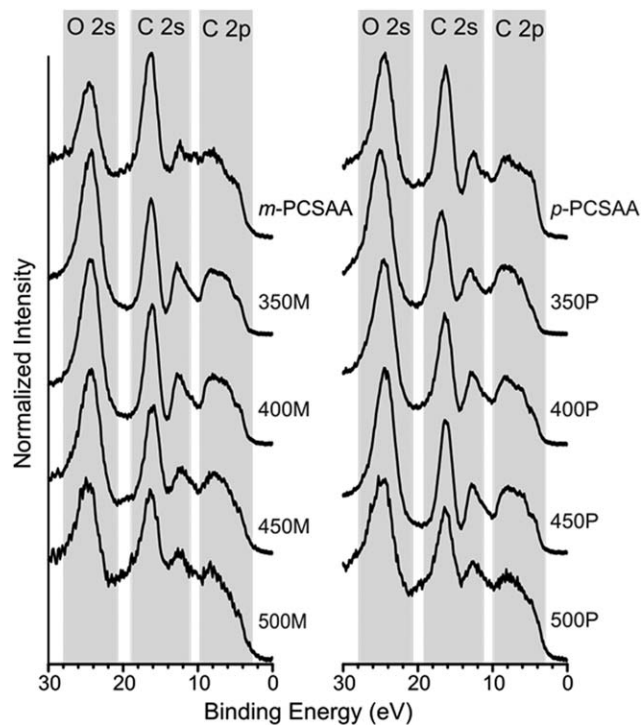


FIGURE 10 Valence band XPS spectra of *p*-PCSAA and *m*-PCSAA before and after heat treatment. The gray boxes highlight the O2s, C 2s, and C 2p bands. The spectra were normalized by the maximum peak intensity of each spectrum for ease of comparison.

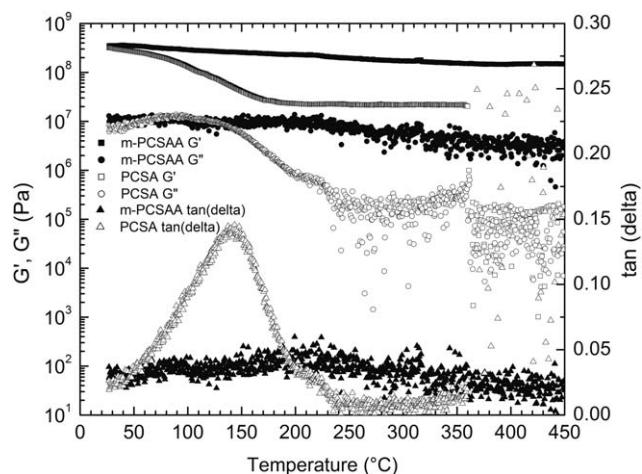


FIGURE 11 G' , G'' , and $\tan \delta$ values of m -PCSAA and PCSA thermosets.

DMA Studies

The mechanical properties of the crosslinked samples of m -PCSAA and PCSA were compared by DMA. The G' , G'' , and $\tan \delta$ of the thermoset samples of both polymers were evaluated by DMA. m -PCSAA and PCSA were fully crosslinked by treatment to 450 and 400 °C, respectively. The ambient G' values of the two thermosets were 350 and 300 MPa, respectively, and the G'' values were 10 and 7 MPa, respectively (Fig. 11). Thus, the ambient G' and G'' of the m -PCSAA thermoset were greater than that of the PCSA thermoset by 16 and 35%, respectively. When the G' and G'' of the m -PCSAA thermoset were determined as a function of temperature under an inert atmosphere, the values gradually decreased to 150 and 2 MPa, respectively, by 450 °C. In comparison, on similar treatment, the G' value of the PCSA thermoset decreased to 20 MPa by 350 °C where upon the sample was found to be unsuitable for measurement. Also, the G'' value of the PCSA thermoset decreased to below 0.1 MPa in the range 350–450 °C. Large drops in both G' and G'' were observed for PCSA thermoset in the temperature range 100–250 °C, which was not the case with the m -PCSAA thermoset. This observation suggested that the m -PCSAA thermoset retained its rigidity over a wide range of temperatures possibly due to the incorporation of aromatic groups, thereby displaying no apparent glass transition temperature. In contrast, the PCSA thermoset seems to be more flexible above ambient temperature and it exhibited a clear glass transition at around 130 °C. Such differences in the material properties of the two thermosets is believed to have originated from the chain stiffening and alterations in the conformation of the polymer chains of m -PCSAA upon incorporation of the aromatic m -DEB group, which result in the initial cycloaddition reactions and a secondary crosslinking via the formation of disilylmethylene bridging entities in the thermoset of m -PCSAA. Further extensive DMA evaluations of both m -PCSAA and p -PCSAA are in progress.

Dielectric Studies

Reports on the dielectric properties of carboranylenesiloxane polymers are virtually non-existent with the only report

being on a vinyl-terminated carboranylenesiloxane monomer, which discovered that there was an anomalous narrowing of the monomer's structural relaxation dispersion function with both increasing temperature and pressure.²² Dielectric spectroscopic studies of m -PCSAA and p -PCSAA, thus, being of great curiosity and interest, were performed at ambient pressure as a function of temperature. Despite the chemically heterogeneous structure of m -PCSAA and p -PCSAA, the segmental dynamics was similar to that of simpler supercooled liquids and polymers. Figure 12 shows representative dielectric loss spectra for m -PCSAA; the spectra for p -PCSAA are qualitatively very similar and are not shown.

Above the glass transition temperature T_g , a single asymmetric peak corresponding to the segmental (α) relaxation is observed for both copolymers. The upturn in dielectric loss at low frequencies is due to dc conduction, which is seen to follow a similar temperature dependence to that of the segmental relaxation and is therefore probably due to residual ionic impurities such as MgBrCl. With decreasing temperature, the segmental relaxation shifts to lower frequencies. The spectra were fitted using a transform in to the frequency domain of the stretched exponential, or Kohlrausch-Williams-Watts (KWW) function.²³

$$\Phi(t) = \exp \left[- \left(\frac{t}{\tau_{\text{KWW}}} \right)^{\beta_{\text{KWW}}} \right]$$

The frequency of maximum loss (related to the timescale of the segmental process, (τ_{KWW})), is plotted in Figure 13 against inverse temperature. The inset shows the temperature dependence of the stretching exponent, β_{KWW} , which quantifies the breadth of the segmental relaxation peak. The temperature dependence of the segmental relaxation frequencies is well described by the Vogel-Tammann-Fulcher equation:²⁴

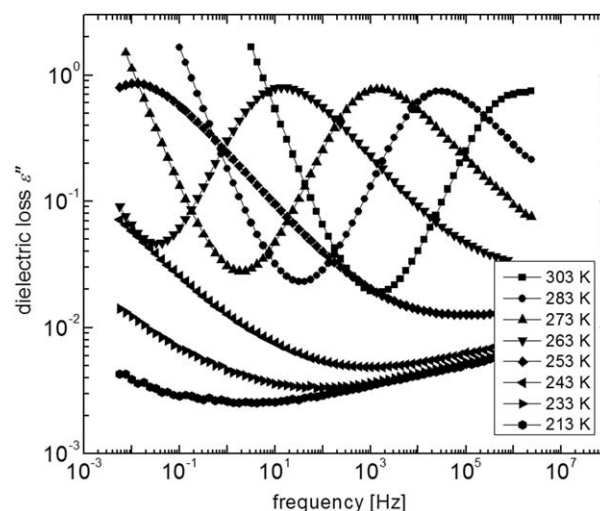


FIGURE 12 Dielectric loss as a function of frequency for m -PCSAA at the indicated temperatures.

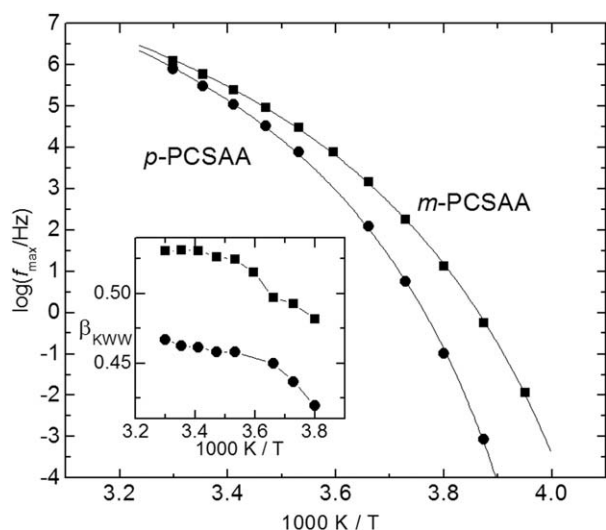


FIGURE 13 Temperature dependence of the segmental relaxation frequencies for *p*-PCSAA and *m*-PCSAA. The inset shows the temperature dependence of the KWW stretching exponent.

$$f_{\max} = f_0 \exp\left(\frac{B}{T - T_0}\right)$$

where f_0 , B , and T_0 are temperature-independent fit parameters.

Comparing the two copolymers, the segmental relaxation is slower for *p*-PCSAA over the entire frequency range, and has a stronger temperature dependence. Extrapolating to a segmental relaxation time of 100 s, a glass transition temperature of 251 and 259 K was obtained for *m*-PCSAA and *p*-PCSAA, respectively. From the data of Figure 13 the fragility m , which quantifies the departure from Arrhenius behavior;²⁵ and is defined as $m = -(\partial \log_{10} f_{\max} / \partial (T_g/T))_{T=T_g}$ was calculated. *m*-PCSAA is less fragile, with $m=117$, compared to $m=132$ for *p*-PCSAA; these are typical values for moderately fragile polymers.

The segmental relaxation peak for *p*-PCSAA is broader than that of *m*-PCSAA, corresponding to smaller values of the KWW stretching exponent (inset to Fig. 13) which indicates larger dynamic heterogeneity. Dynamic heterogeneity has been found to correlate with higher fragility²⁶ and indeed the more dynamically heterogeneous *p*-PCSAA is also the more fragile of the two copolymers.

EXPERIMENTAL

Materials and Instrumentation

BCTMDS-*m*-C obtained from Dexsil Corporation was used without purification. *m*-DEB (97%, Sigma-Aldrich) and *p*-DEB [$>98\%$ (GC), TCI America] were used as received. Ethyl magnesium bromide [EtMgBr, 1.0 M in tetrahydrofuran (THF)], THF (anhydrous, 99.9%), diethyl ether (Et₂O, anhydrous, 99.5%), chloroform-*d* (CDCl₃, 99.6+atom%D), ammonium chloride (NH₄Cl, 99.5+%), granular sodium sulfate (Na₂SO₄, anhydrous, 99+%), activated carbon (Darco® 41-2 mesh, granular) and filter agent, celite®521 (celite) were all

obtained from Sigma-Aldrich and used as received. Molecular weights, relative to poly(methyl methacrylate) standards were obtained using a Water GPC system with RI detection. The measurements were taken at 40 °C with tetrahydrofuran as the mobile phase on two columns connected in series (Shodex KF-806M and Water Styragel HR 4E). TGA were performed on a SDT 2960 simultaneous DTA-TGA analyzer. The differential scanning calorimetry (DSC) studies were performed on a DSC 2920 modulated DSC instrument. Thermal studies (TGA and DSC) were carried out at heating rates of 10 °C/min and argon or air flow rate of 100 cm³/min. Thermal treatment to various temperatures of both PCSAA samples were performed in aluminum pans in an in-house thermal oven under an atmosphere of argon ramping to the respective temperature in 2 h, holding at that temperature for 1 h, and finally, cooling to room temperature in 2 h. FT-IR spectra were obtained as a film on a NaCl plate for *m*-PCSAA and *p*-PCSAA resins and from KBr pellets for the thermally treated PCSAA samples using a Nicolet Magna 750 FT-IR spectrometer. Solution-state ¹H (300 MHz) and ¹³C (75.4 MHz) NMR (both referenced to the internal CDCl₃ standard), ¹¹B NMR (96.3 MHz) (referenced to the internal BF₃·Et₂O standard) and ²⁹Si (59.6 MHz) NMR [referenced to the internal tetramethylsilane (TMS) standard] spectra were acquired on *m*-PCSAA and *p*-PCSAA resins using a Bruker AC-300 spectrometer. The solid-state NMR experiments were performed using a Bruker DMX300 (7.0 T) spectrometer operating at Larmor frequencies of 75.5 and 59.6 MHz for ¹³C and ²⁹Si, respectively. A double-tuned magic-angle spinning probe was used. The 7 mm zirconia rotors containing roughly 60 mg of sample were spun at 6.25 kHz with automatic spinning control. Recycle delays of up to 512 s were used in direct polarization experiments while a recycle delay of 4 s was used in ¹H-¹³C and ¹H-²⁹Si cross polarization experiments. The ²⁹Si, ¹³C, and ¹H $\pi/2$ pulse lengths were 5 μ s and TPPM decoupling of ¹H was used during detection. TMS was used as an external chemical shift reference for both ¹³C and ²⁹Si. X-ray analyses were performed using a Rigaku 18 kW X-ray generator and a high-resolution powder diffractometer. XRD scans of the samples were obtained using Cu K α -radiation from a rotating anode X-ray source. Rheological measurements were performed from ambient temperature to 400 °C in a nitrogen atmosphere on a TA Instruments AR-2000 rheometer in conjunction with an environmental testing chamber for temperature control. Measurements on rectangular solid samples were carried out in the torsion mode at a maximum strain of 2.4×10^{-4} and a frequency of 1 Hz. The samples were prepared in aluminum molds with cavity dimensions of $52 \times 12 \times 2$ mm³ by transferring flowable reaction mixtures into the molds followed by crosslinking in a vacuum desiccator at temperatures up to 500 °C. The storage modulus (G') and loss tangent ($\tan \delta$) were determined as a function of temperature in the 25–450 °C temperature range at a heating rate of 3 °C/min. XPS was performed on the films using a K-Alpha spectrometer (Thermo Scientific) equipped with a microfocusing, monochromatic Al K α source (KE = 1486.6). Survey and high-resolution spectra were collected at 200 and 20 eV

pass energies, respectively, using a spot size of 400 μm . A minimum of three separate spots were analyzed for each of the films after the various treatment conditions. High-resolution spectra were acquired for the Si 2p, C 1s, O 1s, C 2s, C 2p, and O 2s regions to determine the elemental composition of the films and identify the chemical states that were present. Peaks in the high-resolution spectra were fitted with Unifit for Windows (ver. 2011) using a convolution of Lorentzian and Gaussian line shapes to fit the individual components. Dielectric relaxation spectroscopy was carried out using cylindrical electrodes (20-mm diameter) with silica spacers inserted to maintain a constant sample thickness of 40 μm . Spectra were obtained in the frequency range of 10^{-3} – 10^7 Hz using a Novocontrol Alpha analyzer. The temperature was controlled to ± 0.1 K using Delta Design model 9023 oven.

Synthesis of the Poly(carborane-siloxane-*m*-DEB), *m*-PCSAA

EtMgBr (40 mL of 1.0 M soln. in THF; 40 mmol) was transferred to a 250 mL Schlenk flask under argon at room temperature. To this, *m*-DEB (2.64 mL, 20 mmol) was added drop wise. The solution was then brought to reflux when initially a green-gray suspension resulted within 15 min which later turned white in appearance, and the reflux was continued for 2 h. The mixture was subsequently cooled to RT and BCTMDS-*m*-C (8.68 mL, 20 mmol) was added to the mixture over 30 min. The mixture was further refluxed for 2 h and subsequently stirred at RT overnight. An aliquot (~ 0.3 mL) of BCTMDS-*m*-C was added at this point and the mixture was refluxed for an additional hour. The contents were then poured into a saturated NH_4Cl solution (150 mL, aqueous) at 0°C . The resulting two-phase mixture was transferred to a 500-mL separatory funnel and washed with a saturated NH_4Cl (aq) solution until the pH was neutral and, subsequently, twice with distilled H_2O . The clear organic phase was dried over anhydrous Na_2SO_4 and activated carbon in an Erlenmeyer flask. The dried solution was filtered through celite into a round-bottomed flask and concentrated by rotary evaporation. The weight of the crude liquid product was 10.44 g (98 % yield).

Spectroscopic Data of *m*-PCSAA

FT-IR (cm^{-1}): 2961.4, 2595.9, 2156.0, 1593.2, 1569.7, 1475.6, 1407.2, 1259.6, 1164.3, 1078.8, 945.7, 899.1, 857.4, 834.7, 796.1, 703.9, 684.6. ^1H NMR (ppm) (CDCl_3): 7.57–7.19 (m, C_6H_4), 3.5–0.8 (broad, $\text{CB}_{10}\text{H}_{10}\text{C}$), 0.32 (s, CH_3), 0.25 (s, CH_3). ^{13}C NMR (ppm) (CDCl_3): 135.26, 132.21, 128.41, 122.95 (C_6H_4); 103.16, 93.68 ($\text{C}\equiv\text{C}$); 68.33 ($\text{CB}_{10}\text{H}_{10}\text{C}$), 2.08, 0.43 (CH_3). ^{29}Si NMR (ppm) 1.59; $^{-16.78}$ ^{11}B NMR (ppm): $^{-3.08}$, $^{-6.91}$, $^{-8.54}$, $^{-10.51}$, $^{-12.44}$.

DSC Analysis of a Film Sample of *m*-PCSAA in Argon

Exotherms ($^\circ\text{C}$) at 293 (broad, medium) and 393 (sharp, strong). Endotherm ($^\circ\text{C}$) at 196.

TGA Analysis of a Film Sample of *m*-PCSAA: In Argon

5% weight loss at 349 $^\circ\text{C}$. Char yield at 1000 $^\circ\text{C}$: *In Ar* = 84%. *In air*: 93%. DTA: Endotherm ($^\circ\text{C}$) at 218 and exotherms ($^\circ\text{C}$) at 319, 399, 510 and 651.

Synthesis of the Poly(carborane-siloxane-*p*-DEB), *p*-PCSAA

EtMgBr (40 mL of 1.0 M soln. in THF; 40 mmol) was transferred to a 250 mL Schlenk flask under argon at room temperature. White crystals of *p*-DEB (2.52 g, 20 mmol) were dissolved in 5 mL of THF under argon in a separate Schlenk flask and were transferred to EtMgBr soln. drop wise over 30 min. Unlike with *m*-DEB, the formation of a white precipitate resulted *at RT* on complete addition of the Grignard reagent. The suspension was then refluxed for 2 h, subsequently cooled to RT, and BCTMDS-*m*-C (8.68 mL, 20 mmol) was added to the mixture over 10 min. The mixture was refluxed for 2 h when it turned pale reddish brown in the initial 30 min of reflux. The mixture was stirred overnight at RT. An aliquot (~ 0.3 mL) of BCTMDS-*m*-C was added at this point and the mixture was refluxed for an additional hour. The contents were then poured into a saturated NH_4Cl solution (150 mL, aqueous) at 0°C . The resulting two-phase mixture was transferred to a 500-mL separatory funnel and washed with a saturated NH_4Cl (aq) solution until the pH was neutral and, subsequently, twice with distilled H_2O . The clear organic phase was dried over anhydrous Na_2SO_4 and activated carbon in an Erlenmeyer flask. The dried solution was filtered through celite into a round-bottomed flask and concentrated by rotary evaporation. The weight of the crude liquid product was 10.44 g (98 % yield).

Spectroscopic Data of 2

FT-IR (cm^{-1}): 2952.3, 2596.6, 2162.1, 1496.3, 1406.3, 1259.6, 1072.6, 840.5, 796.7. ^1H NMR (ppm) (CDCl_3): 7.39 (s, C_6H_4), 3.5–0.8 (broad, $\text{CB}_{10}\text{H}_{10}\text{C}$), 0.31 (s, CH_3), 0.24 (s, CH_3). ^{13}C NMR (ppm) (CDCl_3): 132.01, 123.21 (C_6H_4); 103.89, 95.28 ($\text{C}\equiv\text{C}$); 68.53 ($\text{CB}_{10}\text{H}_{10}\text{C}$), 2.26, 0.60 (CH_3). ^{29}Si NMR (ppm): 1.59, $^{-16.76}$. ^{11}B NMR (ppm): $^{-2.46}$, $^{-2.80}$, $^{-6.85}$, $^{-8.51}$, $^{-10.52}$, $^{-12.41}$, $^{-14.53}$.

DSC Analysis of a Film Sample of 2 in Argon

Exotherms ($^\circ\text{C}$) at 282 (broad, medium) and 400 (sharp, strong). Endotherm ($^\circ\text{C}$) at 121 and 150.

TGA Analysis of a Film Sample of 2: In Argon

5% weight loss at 400 $^\circ\text{C}$. Char yield at 1000 $^\circ\text{C}$: *In Ar* = 84%. *In air*: 93%. DTA: Endotherms ($^\circ\text{C}$) at 130 and 224 and exotherms ($^\circ\text{C}$) at 292, 412, 500 and 851.

CONCLUSIONS

The incorporation of *m*-DEB or *p*-DEB group in PCSA-like polymers does not detrimentally impact the thermal stability of the resulting polymers. The produced polymers with exceptional thermo-oxidative stability have enhanced mechanical properties as observed from the increased G' and G'' values of the thermoset samples of *m*-PCSAA when compared to that of PCSA. Furthermore, the incorporated aryl groups facilitate a new pathway for crosslinking, that is, cycloaddition of alkynes and aryl groups, as confirmed by FT-IR, ^{29}Si and ^{13}C solid-state NMR, and XPS studies. The cycloaddition

reaction, in turn, facilitate the formation of disilylmethylene bridging entities in the thermoset as it brings the necessary reactive Si—CH₃ groups in close proximity to facilitate the reactions of such Si-bound methyl groups. In addition to the chain stiffening and conformational changes caused by the aromatic group, this secondary crosslinking in the thermosets of *m*-PCSAA and *p*-PCSAA accounts for the enhancement in the *G'* and *G''* values of the thermoset of *m*-PCSAA when compared to the thermoset of PCSA. These encouraging material properties bode well for the material applications of the developed resins as with PCSA.²⁷ The dielectric studies of both *m*-PCSAA and *p*-PCSAA at ambient pressure did not exhibit any anomalous behavior as observed with a vinyl-terminated carboranylenesiloxane polymer at enhanced pressure and temperature. However, it remains to be determined whether similar anomalous trend in the segmental relaxation may manifest in these resins at elevated pressures.

ACKNOWLEDGMENTS

The authors thank the Office of Naval Research for its financial support of this work. They thank Peter Coneski of Chemistry Division, Naval Research Laboratory, Washington, DC, for obtaining the GPC molecular weight data on the polymers.

REFERENCES AND NOTES

- (a) J. F. Ditter, *Inorg. Chem.* **1968**, *7*, 1748–1754; (b) H. A. Schroeder, *Inorg. Macromol. Res.* **1970**, *1*, 45–51; (c) E. Hedaya, J. H. Kawakami, P. W. Kopf, G. T. Kwiatkowski, D. W. McNeil, D. A. Owen, E. N. Peters, R. W. Tulis, *J. Polym. Sci. Polym. Chem. Ed.* **1977**, *15*, 2229–2235; (d) E. N. Peters, D. D. Stewart, J. J. Bohan, R. Moffitt, C. D. Beard, G. T. Kwiatkowski, E. Hedaya, *J. Polym. Sci. Polym. Chem. Ed.* **1977**, *15*, 973–981; (e) E. N. Peters, J. H. Kawakami, G. T. Kwiatkowski, E. Hedaya, B. L. Joesten, D. W. McNeil, D. A. Owens, *J. Polym. Sci. Polym. Chem. Ed.* **1977**, *15*, 723–730; (f) D. D. Stewart, E. N. Peters, C. D. Beard, G. B. Dunks, E. Hedaya, G. T. Kwiatkowski, R. B. Moffitt, J. J. Bohan, *Macromolecules*, **1979**, *12*, 373–377; (g) M. Patel, C. Swain, *Polym. Degrad. Stab.* **2004**, *83*, 539–545; (h) A. C. Swain, M. Patel, J. J. Murphy, *Mater. Res. Symp. Proc.* **2005**, *85*, 363–367; (i) Further examples in Ref. 2.
- P. R. Dvornic, R. W. Lenz, High Temperature Siloxane Elastomers; Huthig & Wepf; Basel, Germany, **1990**.
- (a) D. Bucca, T. M. Keller, *J. Polym. Sci. Part A: Polym. Chem.* **1997**, *35*, 1033–1038; (b) D. Bucca, T. M. Keller, *J. Polym. Sci. Part A: Polym. Chem.* **1999**, *37*, 4356–4359; (c) M. Ichitani, K. Yonezawa, K. Okada, T. Sugimoto, *Polym. J.* **1999**, *31*, 908–912.
- D. D. Stewart, E. N. Peters, C. C. Beard, R. B. Moffitt, G. T. Kwiatkowski, J. J. Bohan, E. Hedaya, *J. Appl. Polym. Sci.* **1979**, *24*, 115–123.
- R. A. Sundar, T. M. Keller, *J. Polym. Sci. Part A: Polym. Chem.* **1997**, *35*, 2387–2394.
- D. J. Lyman, J. Heller, M. Barlow, *Die Makromol. Chem.* **1965**, *84*, 64–79.
- S. Kuroki, K. Okita, T. Kakigano, J.-I. Ishikawa, M. Itoh, *Macromolecules* **1998**, *31*, 2804–2808.
- L. J. Hendersen, T. M. Keller, *Macromolecules* **1994**, *27*, 1660–1661.
- M. K. Kolel-Veetil, H. W. Beckham, T. M. Keller, *Chem. Mater.* **2004**, *16*, 3162–3167.
- (a) H. Sekiguchi, H. C. Kang, G. Teresa, B. Sillion, *Makromol. Chem. Macromol. Symp.* **1991**, *47*, 317–328; (b) H. M. Barentsen, M. van Dijk, P. Kimkes, H. Zuilhof, E. Sudhölter, *Macromolecules*, **1999**, *32*, 1753–1762.
- G. W. King, A. A. G. van Putten, *J. Mol. Spectrosc.* **1978**, *70*, 53–67.
- (a) D. R. Anderson, In *Analysis of Silicones*; A. Lee Smith, Ed.; Wiley-Interscience: New York, **1974**; Chapter 10; (b) L. J. Bellamy, *The Infra-red Spectra of Complex Molecules*, 3rd ed.; Chapman and Hall: London, **1975**; Chapter 20; (c) A. Lee Smith, *Spectrochim. Acta* **1960**, *16*, 87–95.
- R. S. McDonald, *J. Phys. Chem.* **1958**, *62*, 1168–1178.
- (a) D. A. Gordon, A. I. Mikhailov, *J. Photochem. Photobiol. A: Chem.* **1995**, *86*, 253–257; (b) D. A. Gordon, A. I. Mikhailov, *J. Low Temp. Phys.* **2005**, *139*, 675–681; (c) D. A. Gordon, A. I. Mikhaylov, *Low Temp. Phys.* **2009**, *35*, 269–274.
- (a) R. Corriu, P. Gerbier, C. Guerin, B. Henner, R. Fourcade, *J. Organomet. Chem.* **1993**, *449*, 111–118; (b) R. J.-P. Corriu, P. Gerbier, C. Guerin, B. Henner, In *Silicon-Containing Polymers*; R. G. Jones, Ed.; The Royal Society of Chemistry: Cambridge, UK, **1995**.
- (a) U. J. Lorenz, N. Solca, J. Lemaire, P. Maitre, O. Dopfer, *Angew. Chem. Int. Ed. Engl.* **2007**, *46*, 6714–6716; (b) A. Srivatsava, V. B. Singh, *Ind. J. Pure Appl. Phys.* **2007**, *45*, 714–720.
- M. K. Kolel-Veetil, K. P. Fears, S. B. Qadri, C. A. Klug, T. M. Keller, *J. Polym. Sci. Part A: Polym. Chem.* **2012**, *50*, 3158–3170.
- A. S. Jung, R. Navamathavan, K. M. Lee, C. K. Choi, *Surf. Coat. Tech.* **2008**, *202*, 5693–5696.
- J. Riga, J. J. Pireaux, J. P. Boutique, R. Caudano, J. J. Verbiest, *Synth. Met.* **1981**, *4*, 99–112.
- T. Wang, P. M. A. Sherwood, *Chem. Mater.* **1995**, *7*, 1020–1030.
- E. H. Lock, D. Y. Petrovykh, P. Mack, T. Carney, R. G. White, S. G. Walton, R. F. Fernsler, *Langmuir* **2010**, *26*, 8857–8868.
- B. Paulus, M. Paluch, J. Ziolo, M. K. Kolel-Veetil, *J. Phys. Condens. Matter.* **2010**, *22*, 415101.
- G. Williams, D. C. Watts, *Trans. Faraday Soc.* **1970**, *66*, 80–88.
- (a) H. Vogel, *Phys. Z.* **1921**, *22*, 645; (b) G. S. Fulcher, *J. Am. Ceram. Soc.* **1925**, *8*, 339–345; (c) G. Tammann, W. Hesse, *Z. Anorg. Allg. Chem.* **1926**, *8*, 339–347.
- R. Böhmer, K. L. Ngai, C. A. Angell, D. J. Plazek, *J. Chem. Phys.* **1993**, *99*, 4201–4209.
- C. M. Roland, K. L. Ngai, *Macromolecules*, **1991**, *24*, 5315–5319.
- (a) P. E. Pehrsson, L. J. Henderson, T. M. Keller, *Surf. Interface Anal.* **1996**, *24*, 145–151; (b) T. M. Keller, NASA Conference Publications, **2001**, 210427 (Proceedings of the 4th Conference on Aerospace Materials, Processes and Environmental Technology, 2000), 244–249. (c) T. M. Keller, *Carbon*, **2002**, *40*, 225–229; (d) M. K. Kolel-Veetil, T. M. Keller, *PMSE Preprints*, **2005**, *92*, 10–11; (e) M. K. Kolel-Veetil, S. B. Qadri, M. Osofsky, T. M. Keller, *Chem. Mater.* **2005**, *17*, 6101–6107; (f) M. K. Kolel-Veetil, S. B. Qadri, M. Osofsky, T. M. Keller, R. Goswami, S. A. Wolf, *J. Phys. Chem. C* **2007**, *111*, 16878–16882.